



This is a repository copy of *Quasi-active suspension design using magnetorheological dampers*.

White Rose Research Online URL for this paper:
<http://eprints.whiterose.ac.uk/80979/>

Article:

Potter, J.N., Neild, S.A. and Wagg, D.J. (2011) Quasi-active suspension design using magnetorheological dampers. *Journal of Sound & Vibration*, 330 (10). 2201 - 2219. ISSN 0022-460X

<https://doi.org/10.1016/j.jsv.2010.11.029>

Reuse

Unless indicated otherwise, fulltext items are protected by copyright with all rights reserved. The copyright exception in section 29 of the Copyright, Designs and Patents Act 1988 allows the making of a single copy solely for the purpose of non-commercial research or private study within the limits of fair dealing. The publisher or other rights-holder may allow further reproduction and re-use of this version - refer to the White Rose Research Online record for this item. Where records identify the publisher as the copyright holder, users can verify any specific terms of use on the publisher's website.

Takedown

If you consider content in White Rose Research Online to be in breach of UK law, please notify us by emailing eprints@whiterose.ac.uk including the URL of the record and the reason for the withdrawal request.



eprints@whiterose.ac.uk
<https://eprints.whiterose.ac.uk/>

Quasi-active suspension design using magnetorheological dampers

Jack N. Potter*, Simon A. Neild, David J. Wagg

*Department of Mechanical Engineering
University of Bristol
Bristol, BS8 1TR, UK*

Abstract

Quasi-active damping is a method of coupled mechanical and control system design using multiple semi-active dampers. By designing the systems such that the desired control force may always be achieved using a combination of the dampers, quasi-active damping seeks to approach levels of vibration isolation achievable through active damping, whilst retaining the desirable attributes of semi-active systems. In this article a design is proposed for a quasi-active, base-isolating suspension system.

Control laws are firstly defined in a generalised form, where semi-active dampers are considered as idealised variable viscous dampers. This system is used to demonstrate in detail the principles of quasi-active damping, in particular the necessary interaction between mechanical and control systems. It is shown how such a system can produce a tunable, quasi-active region in the frequency response of very low displacement transmissibility.

*Address all correspondence to this author.

Email addresses: jack.potter@bristol.ac.uk (Jack N. Potter), simon.neild@bristol.ac.uk (Simon A. Neild), david.wagg@bristol.ac.uk (David J. Wagg)

Quasi-active control laws are then proposed which are specific for use with magnetorheological dampers. These are validated in simulation using a realistic model of the damper dynamics, again producing a quasi-active region in the frequency response. Finally, the robustness of the magnetorheological, quasi-active suspension system is demonstrated.

Key words: Quasi-active damping, Semi-active damping, MR dampers, Vibration suppression

1. Introduction

The principle of semi-active damping is the control of variable dampers for the purpose of vibration isolation. Semi-active damping has been shown to significantly improve vibration isolation in comparison to passive damping for a range of mechanical and civil engineering applications (see for example [1, 2, 3, 4, 5]). Also, whilst not matching the levels of isolation achievable through active damping, semi-active systems are often attractive in comparison due to their low power consumption, light weight and control stability.

Currently, magnetorheological (MR) dampers are the most widely used class of semi-active damper. They are similar in mechanical design to passive viscous dampers but with micron sized iron particles suspended within the damper fluid. When exposed to a magnetic field, the particles form chains along the lines of magnetic flux, increasing the effective viscosity of the fluid. By varying the current applied to an electromagnet around the orifice of the damper, the damping properties may be controlled.

A number of different approaches have been taken to the design of semi-active controllers. For simple, low-order systems, it is common to design

controllers using intuitive logic specific to the control of semi-active dampers (see for example [6, 7, 8]). Most prominent of these is the sky-hook family of controllers [9], which seek to emulate the response of an inertially grounded damper. Usually this behaviour is approximated by increasing damping when the damping force is acting to dissipate energy from the isolated structure and reducing damping otherwise.

For systems of increased complexity, be it through non-linearity or additional degrees of freedom, it becomes difficult to design controllers based on intuitive logic. As a consequence, for such systems, controllers are usually designed using well established active control techniques, examples include optimal [10, 6] and sliding mode control [11]. Typically, these active controllers output a force demand for the semi-active damper and form an outer-loop of a larger semi-active control scheme. An additional, force feedback, inner-loop controller is then used to command this demanded force in the semi-active damper. A semi-active damper is only able to produce a globally dissipative force, consequently the force demand produced by the active controller cannot always be achieved by the damper. When this occurs, the inner-loop control will set the damping to lowest achievable level in order to minimise the detrimental effect of the damping force on the control action.

Regardless of the approach adopted for controller design, it is this inability of semi-active dampers to produce globally non-dissipative forces which presents the principle restriction on control performance. It is therefore preferable to seek design methods which more explicitly account for, or attempt to negate entirely, the inherent physical limitations of semi-active damper force response.

The authors [12] have previously proposed a semi-active design methodology named quasi-active damping. This approach concerns the design of suspension systems using multiple semi-active dampers which, through a process of coupled mechanical and control system design, allow the desired control force to always be achieved using a combination of the dampers. The motivation for this design method is, by avoiding saturation of the control force, to approach the levels of vibration isolation achievable with active systems whilst retaining the benefits, in terms of stability and low power consumption, associated with semi-active systems.

In this article we present a design for a quasi-active, base-isolating suspension system. Control laws are firstly defined in a generalised form, where semi-active dampers are considered as idealised variable viscous dampers. This system is used to demonstrate in detail the principles of quasi-active damping, in particular the necessary interaction between mechanical and control systems. It is shown how such a system can produce a quasi-active region in the frequency response of very low displacement transmissibility. It is then demonstrated how, through appropriate parameter selection, the size and location of the quasi-active region may be tuned. Furthermore it is shown how the addition of a secondary, closed-loop, control stage can both improve robustness to parameter uncertainty and reduce transmissibility away from the quasi-active region.

Quasi-active control laws are then proposed which are specific for use with magnetorheological dampers. These are validated in simulation using a realistic model of the damper dynamics, again producing a quasi-active region in the frequency response. Finally, the robustness of the magnetorheological,

quasi-active suspension system is demonstrated.

2. Mechanical design

The proposed quasi-active suspension system is shown in Fig. 1(a). The design objective of the system is to support the mass, m_2 , statically whilst isolating it dynamically from the base excitation, r . In this article we will consider the system to be subject to harmonic base excitation such that $r = \Delta \sin \Omega t$. Springs k_1 and k_2 and mass m_1 are design parameters. c_1 and c_2 are semi-active dampers, variable between maximum and minimum values c_{max} and c_{min} respectively. The system has the following governing differential equations

$$m_2 \ddot{x}_2 + (c_1 + c_2) \dot{x}_2 + k_2 x_2 = c_2 \dot{x}_1 + k_2 x_1 + c_1 \dot{r} \quad (1)$$

and

$$m_1 \ddot{x}_1 + c_2 \dot{x}_1 + (k_1 + k_2) x_1 = c_2 \dot{x}_2 + k_2 x_2 + k_1 r. \quad (2)$$

A more conventional mechanical design for a semi-active suspension is shown in Fig. 1(b), in which the isolated mass, m_2 , is connected to the base by a parallel configuration of a spring, k , and semi-active damper, c . The quasi-active design replaces the linear spring with an additional mass, semi-active damper and spring assembly.

It is the inclusion of the mass, m_1 , that is key to enabling quasi-active behaviour. Its function is similar to that of a conventional passive vibration absorber, acting as a sink for the energy driving the system. In this case

however it is also treated as a local store of energy, which may be released, through appropriate control of the damper, c_2 , to aid the isolation of m_2 .

The semi-active dampers, c_1 and c_2 , are to be controlled so that a zero net dynamic force acts on m_2 . To achieve this the spring force of k_2 must be canceled by the dampers. Each semi-active damper can only produce a force on m_2 of direction opposite to that of the relative change in velocity across the damper. In order to cancel the force of k_2 it is therefore necessary for either one or both of the damper velocities to be of opposite direction to the displacement of k_2 at any instant.

Let us first consider the linear response of the system if passively damped. Under this condition the velocity of c_2 will be $\pi/2$ radians in advance of the k_2 displacement. Consequently, the velocity of c_1 must be between $\pi/2$ and π radians in advance of the c_2 velocity in order for either damper force to oppose the k_2 spring force at any instant. The system parameters should be selected to achieve this desired phase relationship.

Once controlled, the damping coefficients will vary positively about the minimum value, c_{min} . Intuitively it can be seen that as damping increases, the relative phase of the two dampers will decrease. Consequently, a suitable starting point for parameter selection is to identify values which produce the upper limit of permissible relative damper phase of π radians, when the damping is set to the minimum value. Once parameters have been chosen, it should then be verified that the relative damper phase does not exceed the lower limit of $\pi/2$ radians at the maximum damping level.

A relative damper phase of π radians may be expressed as follows

$$(\dot{x}_2 - \dot{x}_1)(\dot{x}_2 - \dot{r}) < 0. \quad (3)$$

System parameters are sought which satisfy Eq. (3) at the minimum damping level. However, in order to help locate tractable solutions and noting that c_{min} is assumed to be small, damping shall first be omitted from the parameter selection analysis. The following are analytical steady-state solutions to the differential equations (1) and (2) with damping neglected

$$x_1 = \frac{\Delta k_1(k_2 - m_2\Omega^2) \sin \Omega t}{m_1m_2\Omega^4 - \Omega^2(m_1k_2 + m_2(k_1 + k_2)) + k_1k_2} \quad (4)$$

and

$$x_2 = \frac{\Delta k_1k_2 \sin \Omega t}{m_1m_2\Omega^4 - \Omega^2(m_1k_2 + m_2(k_1 + k_2)) + k_1k_2}. \quad (5)$$

Substituting Eqs. (4) and (5) into Eq. (3), we may obtain a solution for k_2 of

$$k_2 < \frac{m_1m_2\Omega^2 - m_2k_1}{m_1 + m_2}. \quad (6)$$

This also introduces the following constraint for k_1 to ensure a positive value of k_2

$$k_1 < m_1\Omega^2. \quad (7)$$

Note that both the k_1 and k_2 expressions are functions of the excitation frequency, Ω . The control design shall be considered centred about a nominal design frequency used in the selection of k_1 and k_2 . The effect of this design

frequency and corresponding parameter selection will be discussed further in Sec. 3.3.

We shall consider the example of a mass, $m_2 = 2500\text{kg}$, to be isolated from an excitation of amplitude, $\Delta = 0.01\text{m}$, and nominal frequency, $\Omega = 20\text{rad/s}$. Using the guidelines presented in Eqs. (6) and (7), the following parameter values are selected; $m_1 = 500\text{kg}$, $k_1 = 60\text{kN/m}$ and $k_2 = 82\text{kN/m}$. The maximum and minimum damping values are taken as the limits of range for which a Lord RD-1005-1 magnetorheological damper may be linearised, which corresponds approximately to $c_{max} = 10,000\text{Ns/m}$ and $c_{min} = 2000\text{Ns/m}$.

Fig. 2 shows the steady state response of the system at the minimum and maximum damping levels. It can be seen from this figure that, using the chosen parameters, within the range of achievable damping, at any instant at least one damper has a velocity of opposite sign to the displacement of k_2 , thus satisfying the dynamic requirements for quasi-active isolation of m_2 . Note that in Fig. 2 the k_2 displacement has been scaled up by a factor of 10 to aid comparison with the damper velocities.

3. Idealised variable damper control

3.1. Quasi-active control

Control laws for the quasi-active isolation of m_2 must adapt to the directions of the damper velocities, relative to each other and to the displacement of k_2 , at any given moment. For brevity, the following parameters are now introduced

$$A = (x_2 - x_1)(\dot{x}_2 - \dot{x}_1) \tag{8}$$

and

$$B = (x_2 - x_1)(\dot{x}_2 - \dot{r}). \quad (9)$$

Suitable control of the damper coefficients requires consideration of the capability of each damper to resist the k_2 spring force, an attribute related to the signs of A and B . There are four different states of A and B to consider.

State 1, $A < 0$ and $B > 0$:

This corresponds to the force of c_2 acting in the opposite direction to the k_2 spring force and the force of c_1 acting in the same direction as the spring force. The damper, c_2 , can therefore be controlled to cancel the forces of c_1 and k_2 such that the net dynamic force imposed on mass, m_2 , is zero. Setting c_1 to the minimum value and applying a force balance on m_2 produces the following expression for the damper coefficients

$$c_2 = -\frac{k_2(x_2 - x_1) + c_{min}(\dot{x}_2 - \dot{r})}{\dot{x}_2 - \dot{x}_1} \quad (10)$$

$$c_1 = c_{min}.$$

Since Eq. (10) is applied under the condition that $A < 0$ and $B > 0$, the demanded c_2 coefficient will always be positive. It may however be below the minimum achievable value of c_{min} , a condition we will refer to as State 1*. As the c_1 force is acting in the opposite direction to that of c_2 , in this circumstance c_1 may be increased to bring the value of c_2 required to produce a zero net force on m_2 up to a permissible value. A control law for this event may be defined as follows

$$\begin{aligned}
c_1 &= -\frac{k_2(x_2 - x_1) + c_{min}(\dot{x}_2 - \dot{x}_1)}{\dot{x}_2 - \dot{r}} \\
c_2 &= c_{min}.
\end{aligned}
\tag{11}$$

State 2, $A > 0$ and $B < 0$:

Under this condition the c_2 force acts in the same direction as that of k_2 while c_1 produces a force of opposite direction, now permitting c_1 to be controlled to cancel the other forces. Under this condition, setting the coefficients as defined in Eq. (11) will produce a zero net force on m_2 .

As in the previous case, this expression may demand a lower than achievable coefficient for the controlled damper (in this case c_1), a condition we will refer to as State 2*. In a similar approach to the control in State 1*, c_1 may be increased to c_{min} and c_2 , which has velocity of opposite sign, increased accordingly to cancel the force on m_2 . This corresponds to damper coefficients as described in Eq. (10).

State 3, $A < 0$ and $B < 0$:

Here both dampers produce a force opposing that of k_2 . In this situation either damper may be controlled to cancel the k_2 force. To minimise the required damper coefficient, the damper with the highest magnitude of velocity will be controlled and the other coefficient set to the minimum value. Therefore, if the magnitude of the c_1 velocity is higher, Eq. (11) will be applied, else Eq. (10) will be applied (State 3*).

State 4, $A > 0$ and $B > 0$:

In this state neither damper produces a force of opposite direction to that of k_2 . If the system parameters are chosen correctly this should not occur in the steady-state but could occur during transient motion. Under this condition both damping coefficients should be set to the lowest value to minimise the force acting on m_2 .

Controlling the damper coefficients in the manner described above for the different states allows the control logic to be reduced to a simple form, valid regardless of A and B values. For each damper, if the damping coefficient required to produce a zero net force on m_2 , when the other coefficient is set to the minimum value, is greater than c_{min} then that damper should be controlled. In the event that this condition is true for both dampers, the damper with the largest magnitude of velocity is controlled and the other set to c_{min} . These conditions allow the quasi-active controller to be defined in a more concise manner as

$$c_1 = \begin{cases} C, & C > c_{min} > D \text{ or } D > C > c_{min} \\ c_{min}, & \text{otherwise} \end{cases} \quad (12)$$

and

$$c_2 = \begin{cases} D, & D > c_{min} > C \text{ or } C > D > c_{min} \\ c_{min}, & \text{otherwise} \end{cases} \quad (13)$$

where

$$C = -\frac{k_2(x_2 - x_1) + c_{min}(\dot{x}_2 - \dot{x}_1)}{\dot{x}_2 - \dot{r}} \quad (14)$$

and

$$D = -\frac{k_2(x_2 - x_1) + c_{min}(\dot{x}_2 - \dot{r})}{\dot{x}_2 - \dot{x}_1}. \quad (15)$$

Fig. 3 shows the simulated response of x_2 when Eqs. (12) and (13) are applied. Initially the damping coefficients are set to the minimum value and the response is allowed to reach steady-state, in order to establish the desired phase relationships. To avoid drift due to a non-zero velocity at the point when zero net force is achieved, the quasi-active control is applied when $\dot{x}_2 = 0$, which is at a time of approximately 31.5s. This figure shows that the controller functions as designed, isolating m_2 from the excitation, r .

The controlled damping coefficients, c_1 and c_2 , are shown in Figs 4(a) and 4(b) respectively over one steady-state excitation period. From this it is seen that the damping coefficients are always varied within the minimum and maximum limits. Fig. 4(c) shows the damper velocities and k_2 displacement over the same period. This figure shows that, with the control applied, the required relative damper phase is maintained. It should also be noted from this figure that close to the zero crossing of each damper velocity, the other damper is always of appropriate velocity to be controlled. This allows the controller to function without demanding excessively large damping coefficients. Fig. 4 is labeled with the states discussed earlier in this section to illustrate how the controller adapts as these states change.

3.2. Robust control

In order to investigate the sensitivity of the quasi-active controller to parameter uncertainty, an error, ϵ , is introduced to the value of k_2 used by the controller, such that it becomes $k_2(1 + \epsilon)$. The controlled displacement for $\epsilon = 0.05$ is shown in Fig 5, where as before the control is applied at approximately 31.5s. It can be seen that this parameter error reduces the ability of the control to isolate at the excitation frequency and induces a slowly decaying subharmonic transient.

To improve the robustness of the quasi-active controller to parameter uncertainty, a secondary, closed-loop controller is added. The damping coefficients are now defined as the sum of the quasi-active terms given by Eqs. (12) and (13), now denoted as c_{1q} and c_{2q} respectively, and the closed loop terms, c_{1cl} and c_{2cl} . Including maximum and minimum saturation limits, the damping coefficients are expressed as follows

$$c_1 = \begin{cases} c_{1q} + c_{1cl}, & c_{max} \geq (c_{1q} + c_{1cl}) \geq c_{min} \\ c_{max}, & (c_{1q} + c_{1cl}) > c_{max} \\ c_{min}, & (c_{1q} + c_{1cl}) < c_{min} \end{cases} \quad (16)$$

and

$$c_2 = \begin{cases} c_{2q} + c_{2cl}, & c_{max} \geq (c_{2q} + c_{2cl}) \geq c_{min} \\ c_{max}, & (c_{2q} + c_{2cl}) > c_{max} \\ c_{min}, & (c_{2q} + c_{2cl}) < c_{min} \end{cases} \quad (17)$$

The closed-loop control terms are given by Eqs. (18) and (19). These controllers are similar in form to classical proportional plus derivative control. Since a damping coefficient is the control output, the resulting force on m_2

will be of opposite direction to the damper velocity. Consequently, the sign of the output is corrected to account for the direction of the damper velocity. Although negative values for c_1 and c_2 are physically unobtainable, due to the positive quasi-active components, negative closed loop components can be permissible.

$$c_{1cl} = \begin{cases} |k_p x_2 + k_d \dot{x}_2|, & (k_p x_2 + k_d \dot{x}_2)(\dot{x}_2 - \dot{r}) \geq 0 \\ -|k_p x_2 + k_d \dot{x}_2|, & \text{otherwise} \end{cases} \quad (18)$$

$$c_{2cl} = \begin{cases} |k_p x_2 + k_d \dot{x}_2|, & (k_p x_2 + k_d \dot{x}_2)(\dot{x}_2 - \dot{x}_1) \geq 0 \\ -|k_p x_2 + k_d \dot{x}_2|, & \text{otherwise} \end{cases} \quad (19)$$

Primarily it is the derivative term that is responsible for improving the systems robustness, acting to dissipate energy from m_2 by providing a force resistant to its velocity. The proportional term is added to encourage m_2 to oscillate about zero, rather than its displacement at the time the control is applied (as was seen in Fig. 3). The addition of this controller also negates the need for the control to be applied when $\dot{x}_2 = 0$, as the derivative term will act against any non-zero velocity.

Increasing the magnitude of k_p relative to k_d increases the rate of decay of the low frequency transience at the expense of steady-state amplitude. The control gains, k_p and k_d , are empirically selected as 10^3 and 5×10^6 respectively to provide a balance between steady-state and transient response. While these gains may appear large, as we are seeking to control to very low amplitudes, the resulting closed-loop damping coefficients will be small.

The response of x_2 , for $\epsilon = 0.05$, with the closed-loop control terms added is shown as a dashed line in Fig. 5. It can be seen that the addition of the

closed-loop terms removes both the subharmonic response and the majority of the response at the excitation frequency. The closed-loop damping components are shown in Fig. 6 while Fig. 7 shows the controlled damping coefficients, including both quasi-active and closed-loop components. From these figures it is clear that the quasi-active component (see Fig. 4) remains the dominant control term and that only a comparatively small closed-loop component is required to compensate for parameter uncertainty in the quasi-active control.

3.3. Frequency response

So far in this paper the system's response has only been examined at the nominal design frequency of $\Omega = 20\text{rads/s}$. The response will now be considered at frequencies away from this value. By obtaining values of steady-state displacement transmissibility from a range of single frequency excitations, plots of frequency response are obtained. Fig. 8 shows the steady-state transmissibility of the quasi-active suspension system, in comparison to the passively damped system.

At lower frequency the phase relationships necessary for quasi-active control are not present, recall that the onset frequency of the required relative damper phase was determined through the selection of k_1 and k_2 . At these frequencies, the closed-loop control is dominant, producing isolation comparable with that of conventional semi-active damping.

As frequency increases, the required $\pi/2$ radian relative damper phase becomes established at which point the transmissibility rapidly decreases, producing a quasi-active region in the frequency response. Theoretically the transmissibility is zero within the quasi-active region however, as a conse-

quence of numerical error, the computed values are in the order of 10^{-17} . It should be noted that, practically, the transmissibility in this region will be limited by factors such as sensor resolution.

The existence of an upper limit to the quasi-active region is not due to a loss of required damper phase, but rather can be explained by examining the amplitudes of the damper velocities. Within the quasi-active region, the amplitude of x_2 is very low and so the velocity of c_1 is equal to approximately $-\dot{r}$. As frequency increases through the quasi-active region, the amplitude of the c_1 velocity increases and, as can be seen in Fig. 9, the amplitudes of the c_2 velocity and k_2 displacement decrease.

Fig. 10 shows the quasi-active damping components, k_2 displacement and damper velocities at an excitation frequency, Ω , of 25rads/s, which is just beyond the upper limit of the quasi-active region. When compared to the equivalent figure (Fig. 4) at an excitation frequency within the quasi-active region, it can be seen that the amplitude of the c_1 velocity has increased relative to that of c_2 . It is also observed that, at the higher frequency, a greater proportion of the period is spent in state 2*. This state occurs when the c_1 damping force is of opposite direction to the k_2 spring force but is also of greater magnitude at the minimum damping level, requiring c_2 to be increased to achieve a zero net force on m_2 . As state 2* is moved through, the magnitude of the c_2 velocity decreases, thereby increasing the damping coefficient required to cancel the c_1 force. The c_2 velocity eventually decreases to the point at which the c_2 coefficient becomes saturated at c_{max} , preventing a zero net force being achieved of m_2 . This saturated region is labeled as α in Fig. 10.

Similarly, the quasi-active control is unable to function as intended due to the increased c_1 velocity in the region labeled β . Here both dampers produce a force of opposite direction to that of k_2 . However, the magnitude of the c_1 velocity relative to the k_2 displacement is large enough that, at the minimum damping level, the damping forces are of larger magnitude than the spring force. Consequently both damping coefficients are saturated at c_{min} to minimise the resulting net force.

Conditions α and β are both caused by the increase in c_1 velocity with frequency resulting in a damping force of too large a magnitude at c_{min} . The upper limit of the quasi-active region is therefore restricted by the minimum obtainable damping value.

As a comparison to more conventional passive and semi-active base-isolating suspension designs, the frequency response of a typical single degree of freedom system, such as that shown in Fig. 1(b) is presented. As is the case for the quasi-active system, parameters may be chosen to optimise the response within a desired frequency range. To provide the most direct comparison, the spring stiffness, k , is selected such that the undamped natural frequency of the system matches that first undamped natural frequency of the quasi-active system. This corresponds to a value of $k=34\text{kN/m}$. The response of this system is examined when passively damped and when subject to an on-off sky-hook semi-active controller. This control law may be expressed as follows

$$c = \begin{cases} c_{max}, & \dot{x}_2(\dot{x}_2 - \dot{r}) > 0 \\ c_{min}, & \text{otherwise.} \end{cases} \quad (20)$$

The implementation of the sky-hook controller is not intended as a bench-

mark of the best achievable semi-active performance, but rather as the general indication of the comparative level of semi and quasi-active isolation.

The steady-state peak displacement and acceleration frequencies response of the passive, sky-hook and quasi-active systems are shown in Fig. 11. As is well reported, an increased passive damping coefficient provides improved transmissibility below and close to the natural frequency, at the expense of poorer higher frequency performance. In comparison to passive damping, sky-hook control provides improves performance at lower frequency but is observed to be inferior to light passive damping at higher frequency. Between the first natural frequency and the onset of the quasi-active region performance is seen to be comparable between the quasi-active and sky-hook systems, albeit with slight increased displacement transmissibility for the quasi-active system due to the second natural frequency. It is clear from Fig. 11, however, that within the quasi-active region, the very low levels of transmissibility achieved using the quasi-active system cannot be approached by conventional passive and semi-active systems.

The level of transmissibility within the quasi-active region is comparable with that which may be achieved by a fully active system employing a similar stiffness cancelling control method and assuming perfect force control and exact knowledge of system parameters and states. It is well documented in the literature (for example see [17]), that semi-active systems require input power several orders of magnitude lower than active systems. It is reasonable to presume that due to the additional semi-active damper, the input power of the quasi-active system will be approximately twice that of a conventional semi-active system. Nevertheless, the performance within the quasi-active

region is still achieved at a fraction of the input power required by an active system.

In order to examine the influence of parameter uncertainty on the frequency response of the quasi-active suspension system, transmissibility plots are obtained for a range of ϵ values and are shown in Fig. 12. From this figure it can be seen that outside of the quasi-active region, where the closed-loop control is dominant, the response is unaffected by parameter uncertainty. Within the quasi-active region, an increase in the magnitude of ϵ reduces the effectiveness of the isolation. However, although increased by parameter uncertainty, the achieved transmissibilities are still several orders of magnitude lower than may be obtained through passive or conventional semi-active damping.

It is desirable to be able to tune the location and width of the quasi-active region. The precise affect of the system parameters on the frequency response is complicated. However, it was found that generally an increase in m_1 will increase the width of the quasi-active region. An appropriate guide for parameter selection is therefore to firstly choose m_1 to determine the width and then select k_1 and k_2 using Eqs. (6) and (7) to choose the onset frequency of the quasi-active region. To illustrate this process, Fig. 13 shows the frequency response for a range of system parameters.

4. Magnetorheological damper control

In the previous section, a quasi-active controller was proposed for the generalised form of semi-active damper. In this section quasi-active control will be considered in a form specific to the application of magnetorheological

dampers.

4.1. Mechanical model

The mechanical design of the suspension system and parameter selection remains as described in Sec. 2, but now the variable dampers, c_1 and c_2 , are replaced with magnetorheological dampers which produce forces of F_1 and F_2 respectively. The system's equations of motion may now be written as

$$m_2\ddot{x}_2 + k_2(x_2 - x_1) + F_1 + F_2 = 0 \quad (21)$$

and

$$m_1\ddot{x}_1 + k_1(x_1 - r) - k_2(x_2 - x_1) - F_2 = 0. \quad (22)$$

The dynamics of the MR dampers are represented in simulation using the model proposed by Spencer et al. [13]. This model, which incorporates the Bouc-Wen model of hysteresis, is often adopted in the literature and has been shown to accurately capture the non-linear dynamics of MR dampers (see for example [14, 15, 11]). The equations of the n^{th} MR damper are given by Eq. (23) and illustrated in Fig. 14. Note that some of the nomenclature has been changed to distinguish the damper model parameters from those of the suspension system. V_n is the applied voltage, variable between minimum and maximum limits of V_{min} and V_{max} respectively. The damper displacements are $x_{D1} = x_2 - r$ and $x_{D2} = x_2 - x_1$.

$$\begin{aligned}
\dot{y}_n &= (\alpha_n z_n + k_{0D}(x_{Dn} - y_n) + c_{0Dn}\dot{x}_{Dn}) / (c_{0Dn} + c_{1Dn}) \\
\dot{z}_n &= -\gamma|\dot{x}_{Dn} - \dot{y}_n||z_n|^{k-1}z_n - \mu(\dot{x}_{Dn} - \dot{y}_n)|z_n|^k + A(\dot{x}_{Dn} - \dot{y}_n) \\
F_n &= c_{1Dn}\dot{y}_n + k_{1D}(x_{Dn} - x_0) \\
\alpha_n &= \alpha_a + \alpha_b u_n \\
c_{1Dn} &= c_{1a} + c_{1b} u_n \\
c_{0Dn} &= c_{0a} + c_{0b} u_n \\
\dot{u}_n &= -\eta(u_n - V_n)
\end{aligned} \tag{23}$$

The parameters used are those obtained by Lai et al. [11] for a Lord RD-1005-1 MR damper and are shown in Table 5. Since we are considering the dynamic response of the suspension system about the static deflection, the static offset in stiffness, x_0 , is taken as zero.

4.2. Damper force control

The magnetorheological damper formulation of quasi-active control will output a force demand, F_{dn} , for each damper rather than a damping coefficient, as was the case for with variable damper control. A separate force feedback controller, outputting the damper control voltage, is then employed in order to achieve the desired force demand for each damper. The force controller for the n^{th} damper is given by Eq. (24). This is a proportional controller, with gain, G , which has the addition of a sign correction to the output voltage to allow for the fact that a positive increase in voltage will increase the magnitude of the control force, regardless of its direction. This method of force control was first proposed by Sims et al.[16] for the control of electro-rheological dampers and has since been applied to MR dampers [11].

$$V_n = \begin{cases} G(F_{dn} - F_n)\text{Sign}(F_n), & V_{max} \geq G(F_{dn} - F_n)\text{Sign}(F_n) \geq V_{min} \\ V_{max}, & G(F_{dn} - F_n)\text{Sign}(F_n) > V_{max} \\ V_{min}, & \text{otherwise.} \end{cases} \quad (24)$$

To demonstrate the performance of the force controller, a sinusoidal displacement of $x_D = \Delta \sin \Omega t$ is applied to the damper model and the force demand is set to $F_d = c\dot{x}_D$ in an effort to linearise the damper response to a viscous damping coefficient of $c=5000$ Ns/m. Fig. 15 shows the force-velocity response of the controlled damper for $G = 0.1$. It can be seen that, away from velocity zero crossing, the control is very effective, however close to zero velocity the control cannot compensate for the hysteresis. In application to conventional semi-active control, this uncontrollable region would restrict performance. However for the case of quasi-active damping, as previously discussed and shown in Fig. 4, close to the zero crossing of each damper velocity, the other damper velocity is always of the required direction to cancel the k_2 spring force. Consequently, within the quasi-active region of the frequency response, control will not be required of either damper within this uncontrollable velocity region.

4.3. Quasi-active control

Each damper force demand will contain quasi-active and closed loop components of F_{dnq} and F_{dcl} respectively, such that

$$F_{dn} = F_{dnq} + F_{dcl}. \quad (25)$$

The disparity between achieved and demanded damper forces allows for a more elegant formulation of the quasi-active control laws than could be achieved for the idealised variable damper control case. The quasi-active components of the force demands are defined as follows

$$F_{d1q} = -k_2(x_2 - x_1) - F_2 \quad (26)$$

and

$$F_{d2q} = -k_2(x_2 - x_1) - F_1. \quad (27)$$

By substituting Eqs. (25), (26) and (27) into Eq. (24), it can be seen that the control error in each force controller becomes

$$F_{d1} - F_1 = F_{d2} - F_2 = -k_2(x_2 - x_1) - F_1 - F_2 + F_{dcl}. \quad (28)$$

Each damper voltage is therefore controlled so that a net force of F_{dcl} is produced on m_2 . The saturation limits in Eq. (24) in conjunction with the quasi-active force demands will cause the controller to adapt to the changing system states in a manner broadly following the same logic as was discussed for variable linear damper control in Sec. 3.2.

For clarity in the explanation of the quasi-active control behaviour and to provide a more direct comparison to the logic of the variable linear damper control, the comparatively small closed-loop terms, whose inclusion produces only a slight deviation from the dominant control process, are omitted from the following discussion.

As a consequence of damper stiffness and hysteresis, the zero crossing of damper force no longer precisely corresponds to the zero crossing of damper

velocity, for the MR damper system it is therefore pertinent to discuss control logic in terms of the direction of damper force rather than velocity.

Consider the case that the force generated by damper 1, F_1 , is not of the correct direction to cancel the k_2 spring force but the damper 2 force, F_2 , is. This is analogous to State 1 considered in Sec. 3.2 for the variable linear damper system. The force controller will saturate V_1 at V_{min} and F_{2dq} will be selected to achieve a zero net force on m_2 . Since the spring force is being canceled, the force demand, F_{d1q} , will become that achieved by $V_1 = V_{min}$. Consequently, throughout the time when V_1 is not controlled to cancel k_2 , F_1 will continue to track F_{d1q} .

Now consider the case that the force directions are as above, however at $V_1 = V_2 = V_{min}$ the magnitude of F_2 is greater than that of the combined k_2 and c_1 forces, a situation analogous to State 1*. Now V_2 will become saturated at V_{min} and F_{d1q} selected to cancel the other forces. In a similar manner to the previous case, as a zero net force is achieved on m_2 with V_2 at the minimum value, the quasi-active force demand for damper 2, F_{d2q} , will become that achieved by $V_2 = V_{min}$.

By similar mechanisms, the controller will automatically adapt to the changing system states in manner consistent with the quasi-active control logic detailed in Sec 3.2, producing continuous force demands which are always of achievable direction.

The closed-loop component of the force demand is similar in form and function to that proposed for variable damper control and is defined as follows, where k_d and k_p are derivative and proportional gains

$$F_{dcl} = k_d \dot{x}_2 + k_p x_2. \quad (29)$$

The interaction between the control systems is shown schematically in Fig. 16.

The entire control system requires knowledge of the two damper forces, relative displacement between masses m_1 and m_2 and the absolute velocity and displacement of m_2 . In a practical implementation of the proposed system, the damper forces and relative displacement would be directly measurable using force and displacement transducers. The absolute states, which are required by most semi-active controllers, are more difficult to measure directly but may be inferred through integration of an acceleration measurement.

The only system parameter required by the controller is the spring constant, k_2 . The controller could however be re-expressed in terms of the force of spring k_2 , rather than its displacement and stiffness. This spring force could then be measured directly, removing the requirement for any explicit parameter knowledge in the controller.

Fig. 17 shows the controlled response of x_2 when excited at the design frequency, $\Omega = 20\text{rads/s}$, with closed-loop of gains of $k_p = 10^6$ and $k_d = 10^7$. The system is first run to steady state with $V_1 = V_2 = V_{min}$, before the quasi-active control is switched on at a time of approximately 32s. It can be seen that, as with the variable damper control, the control isolates m_2 from the base excitation very effectively. It should be noted that due to the imperfect force control, even with no parameter uncertainty, the closed-loop component is required to avoid inducing the kind of subharmonic response

seen in Fig. 5.

The demanded and achieved damper forces are shown over one steady state excitation period in Fig. 18. The achieved forces are seen to very closely track the demands. This level of force control is only possible because in the region of uncontrollable damper velocity, the force demand is equal to the damping force at the minimum voltage.

Fig. 19 shows the controlled damper voltages over the same excitation period. It can be seen that, qualitatively, for most of the period the variation of voltages closely matches that of the controlled damping coefficients shown in Fig. 4 for the variable linear damper control. During states 3 and 3* however, where both dampers produce a force opposing the spring force, the voltages distribute the force required to cancel k_2 between the two dampers, whereas the variable linear damper control uses only one of the dampers.

It is worth making clear at this stage that it is not necessary to run the system to a passive steady-state before applying the quasi-active control. That has been the convention so far in this paper to help emphasise the difference in amplitude between the passive and quasi-active response. To illustrate this point, Fig. 20 shows the displacement response with the control applied at zero initial conditions. It can be seen that the quasi-active control begins to function effectively within a single excitation period, after which point the amplitude decays towards zero. Also shown in Fig. 20 is the controlled displacement when the proportional closed loop term is omitted, it can be seen that this allows the steady-state to be achieved more rapidly but with the loss of a zero static position.

The steady-state frequency response of the quasi-active, MR suspension

system is shown in Fig. 21. As before, a quasi-active region of very low displacement transmissibility is present. At frequencies below the quasi-active region, isolation is again seen comparable to that of conventional semi-active damping, due to the closed-loop controller. The lower limit of the quasi-active region (triggered by the onset of $\pi/2$ radian relative damper phase) agrees closely with that of the variable damper control. The upper limit, however, is higher for the MR damper system. For the variable damper control, c_{min} was taken as the lower limit for which the MR damper may be effectively linearised. Though not a linear response, the MR damper will produce a lower magnitude force at V_{min} than c_{min} for a given velocity. Consequently, as the upper limit of the quasi-active region is restricted by the minimum damping force of damper 1, this limit is increased for MR damper control.

As before, the robustness of the system to parameter uncertainty is examined by introducing an error ϵ to the controller value of k_2 such that it becomes $k_2(1 + \epsilon)$. Fig. 22 shows the displacement transmissibility of the system for various ϵ values. The figure shows the system to be robust to parameter uncertainty, with parameter error only marginally increasing transmissibility in the quasi-active region.

The proposed system is designed to provide very precise isolation within a desired frequency range. In a practical implementation it is unrealistic to expect a purely sinusoidal base excitation. A rigorous study of the system's sensitivity to additional excitation frequency content should be a consideration of future work and is beyond the scope of this paper. However, to provide an initial qualitative assessment, a higher frequency stochastic com-

ponent is added to a 20 rad/s base excitation. The displacement response of the quasi-active system and base displacement are shown in Fig. 23. As a reference point, the response of an MR damper sky-hook system, switching between v_{min} and v_{max} , is also shown (simulated using the same damper model and parameters as the quasi-active system and the single degree-of-freedom suspension parameters given in Sec. 3.3).

It can be seen that the additional higher frequency component produces a slight degradation in the quasi-active control performance. This is caused by the occurrence of instances at which the velocity relationships necessary for correct functioning of the quasi-active control are briefly lost. However, due to action of the secondary, closed-loop controller, these instances trigger only a slow, low-amplitude transient response. The quasi-active system is still seen to provide a considerable reduction in vibration in comparison to the sky-hook system.

5. Conclusions

In this article a design is proposed for a quasi-active, base-isolating suspension system. Quasi-active damping is a method of design using multiple semi-active dampers which attempts to compensate for the inability of semi-active dampers to produce globally non-dissipative forces. The principle behind quasi-active damping is that, through applying a process of coupled mechanical and control design, the desired control force can always be achieved using a combination of the semi-active dampers. The motivation of this design methodology is to approach levels of vibration isolation achievable through active damping, whilst retaining the desirable attributes

of semi-active systems.

Initially the semi-active dampers are considered in an idealised form as variable viscous dampers. The mechanical suspension design and quasi-active control laws for variable dampers are proposed and validated in simulation. This system is used to demonstrate in detail the principles of quasi-active damping, in particular the control logic and the necessary interaction between mechanical and control systems. It is shown that the proposed system produces a quasi-active region in the frequency response of very low displacement transmissibility. The location and width of this quasi-active region and how it may be tuned through selection of the system parameters is discussed. It is also shown how the addition of a secondary, closed-loop controller can both improve the system's robustness of parameter uncertainty and reduce transmissibility outside of the quasi-active region.

Quasi-active control laws are then proposed which are specific for use with magnetorheological dampers. These are validated in simulation using a realistic model of the damper dynamics, again producing a quasi-active region in the frequency response. Finally, the robustness of the magnetorheological, quasi-active suspension system is demonstrated.

Acknowledgments

The authors would like to acknowledge the support of the EPSRC. Jack Potter is supported by an EPSRC DTA.

References

- [1] Seung-Bok Choi, Moo-Ho Nam, and Byung-Kyu Lee. Vibration Control of a MR Seat Damper for Commercial Vehicles. *Journal of Intelligent Material Systems and Structures*, 11(12):936–944, 2000.
- [2] Mehdi Ahmadian and Christopher A. Pare. A Quarter-Car Experimental Analysis of Alternative Semiactive Control Methods. *Journal of Intelligent Material Systems and Structures*, 11(8):604–612, 2000.
- [3] Hui Li, Min Liu, Jinhai Li, Xinchun Guan, and Jinping Ou. Vibration control of stay cables of the shandong binzhou yellow river highway bridge using magnetorheological fluid dampers. *Journal of Bridge Engineering*, 12(4):401–409, 2007.
- [4] Erik A. Johnson, Greg A. Baker, Jr. B. F. Spencer, and Yozo Fujino. Semiactive damping of stay cables. *Journal of Engineering Mechanics*, 133(1):1–11, 2007.
- [5] S J Dyke, B F Spencer-Jr, M K Sain, and J D Carlson. An experimental study of mr dampers for seismic protection. *Smart Materials and Structures*, 7(5):693–703, 1998.
- [6] Laura M. Jansen and Shirley J. Dyke. Semiactive control strategies for mr dampers: Comparative study. *Journal of Engineering Mechanics*, 126(8):795–803, 2000.
- [7] Jack N. Potter, Simon A. Neild, and David J. Wagg. Generalisation and optimisation of semi-active, on-off switching controllers for single degree-

- of-freedom systems. *Journal of Sound and Vibration*, 329(13):2450 – 2462, 2010.
- [8] G. Verros, S. Natsiavas, and G. Stepan. Control and dynamics of quarter-car models with dual-rate damping. *Journal of Vibration and Control*, 6(7):1045–1063, January 2000.
- [9] Crosby M. J. Karnopp, D. C. and R. Harwood. Vibration control using a semi-active force generator. *Trans. ASME, J. Eng. for Industry*, 96:2:619–626, 1974.
- [10] R.S. Prabakar, C. Sujatha, and S. Narayanan. Optimal semi-active preview control response of a half car vehicle model with magnetorheological damper. *Journal of Sound and Vibration*, 326:400–420, 2009.
- [11] Chun-Yu Lai and W.H Liao. Vibration control of a suspension system via a magnetorheological fluid damper. *Journal of Vibration and Control*, 8(4):527–547, 2002.
- [12] Jack N. Potter, Simon A. Neild, and David J. Wagg. Quasi-active damping. *Proceedings of the ASME 2009 International Design Engineering Technical Conferences & Computers and Information in Engineering Conference IDETC/CIE 2009*, 2009.
- [13] B. F. Spencer-Jr., S. J. Dyke, M. K. Sain, and J. D. Carlson. Phenomenological model for magnetorheological dampers. *Journal of Engineering Mechanics*, 123(3):230–238, 1997.
- [14] Xiao Qing Ma, S. Rakheja, and Chun-Yi Su. Development and relative

- assessments of models for characterizing the current dependent hysteresis properties of magnetorheological fluid dampers. *Journal of Intelligent Material Systems and Structures*, 18:487–502, 2007.
- [15] S J Dyke, B F Spencer-Jr, M K Sain, and J D Carlson. Modeling and control of magnetorheological dampers for seismic response reduction. *Smart Materials and Structures*, 5(5):565–575, 1996.
- [16] N D Sims, R Stanway, D J Peel, W A Bullough, and A R Johnson. Controllable viscous damping: an experimental study of an electrorheological long-stroke damper under proportional feedback control. *Smart Materials and Structures*, 8(5):601–615, 1999.
- [17] I Ballo. Comparison of the properties of active and semiactive suspension. *International Journal of Vehicle Mechanics and Mobility*, 45(11):1065–1073, 2007.

List of Figures

1	Mechanical models of (a) Quasi-active suspension system (b) Semi-active suspension system	36
2	Steady state passive response for (a) $c_1 = c_2 = c_{min}$; (b) $c_1 = c_2 = c_{max}$: $-\cdot-\cdot-$ $10(x_2 - x_1)$ [m], $---$ $(\dot{x}_2 - \dot{r})$ [m/s], $---$ $(\dot{x}_2 - \dot{x}_1)$ [m/s].	37
3	Controlled displacement transmissibility	38
4	Steady-state controlled response (a) c_1 damping coefficient, (b) c_2 damping coefficient , (c) Damper velocities and k_2 displacement; $-\cdot-\cdot-$ $10(x_2 - x_1)$ [m], $---$ $(\dot{x}_2 - \dot{r})$ [m/s], $---$ $(\dot{x}_2 - \dot{x}_1)$ [m/s].	39
5	Controlled displacement for $\epsilon = 0.05$; $---$ Quasi-active control, $---$ Quasi-active + closed loop control.	40
6	Closed-loop control terms for $\epsilon = 0.05$; (a) c_1 closed-loop coefficient (b) c_2 closed-loop coefficient.	41
7	Controlled damping coefficients for $\epsilon = 0.05$, including quasi-active and closed-loop components (a) c_1 coefficient (b) c_2 coefficient.	42
8	Displacement transmissibility; $---$ Quasi-active control, $-\cdot-\cdot-$ Passive damping ($c_1 = c_2 = c_{max}$), $---$ Passive damping ($c_1 = c_2 = c_{min}$).	43

9	Controlled frequency response of k_2 displacement and damper velocity amplitudes; ——— $(\dot{x}_2 - \dot{x}_1)$ [m/s], - - - $(\dot{x}_2 - \dot{r})$ [m/s], - · - · - $(x_2 - x_1)$ [m].	44
10	Steady-state controlled response at $\Omega = 25$ rad/s (a) c_{1q} damping coefficient, (b) c_{2q} damping coefficient, (c) Damper velocities and k_2 displacement; - · - · - $10(x_2 - x_1)$ [m], - - - $(\dot{x}_2 - \dot{r})$ [m/s], ——— $(\dot{x}_2 - \dot{x}_1)$ [m/s].	45
11	Steady-state frequency response of (a) displacement transmissibility (b) acceleration transmissibility; ——— Quasi-Active, - · - · - Single DOF passive $c = 10,000$ Ns/m, Single DOF passive $c = 2,000$ Ns/m, - - - Sky-hook.	46
12	Displacement transmissibility of quasi-active suspension system; ——— $\epsilon = 0$, - · - · - $\epsilon = 0.01$, - · - · - $\epsilon = 0.05$, - - - $\epsilon = -0.05$	47
13	Displacement transmissibility of quasi-active suspension system; - · - · - $m_1 = 250$ kg, $k_1 = 47$ kN/m, $k_2 = 50$ kN/m, - - - $m_1 = 375$ kg, $k_1 = 25$ kN/m, $k_2 = 46$ kN/m, - · - · - $m_1 = 500$ kg, $k_1 = 94$ kN/m, $k_2 = 91$ kN/m, ——— $m_1 = 750$ kg, $k_1 = 51$ kN/m, $k_2 = 64$ kN/m.	48
14	Mechanical model of magnetorheological damper [13]	49
15	Force-velocity response of feedback linearised MR damper; ——— Achieved force, - - - Demanded force	50

16	Illustration of control and mechanical systems.	51
17	Controlled displacement of quasi-active MR suspension system	52
18	Steady-state demanded and achieved damper forces of quasi-active MR suspension system for $\Omega = 20\text{rads/s}$ (a) MR Damper 1; ——— F_1 , - - - F_{d1} (b) MR damper 2; ——— F_2 , - - - F_{d2}	53
19	Steady-state damper control voltages of quasi-active MR suspension system for $\Omega = 20\text{rads/s}$ (a) V_1 (b) V_2	54
20	Controlled displacement of quasi-active MR suspension system from zero initial conditions for $\Omega = 20\text{rads/s}$; - - - Full control, ——— Proportional closed-loop control omitted.	55
21	Displacement transmissibility of MR suspension system; ——— Quasi-active control, - - - Passive, $V_1 = V_2 = V_{min}$, - . . . - Passive, $V_1 = V_2 = V_{max}$	56
22	Displacement transmissibility of quasi-active MR suspension system; ——— $\epsilon = 0$, - - - $\epsilon = 0.05$, - . . . - $\epsilon = -0.05$	57
23	Response to excitation of 20 rad/s and higher frequency stochastic component; ——— base excitation r , - - - x_2 displacement of MR sky-hook system, x_2 displacement of MR quasi-active system.	58

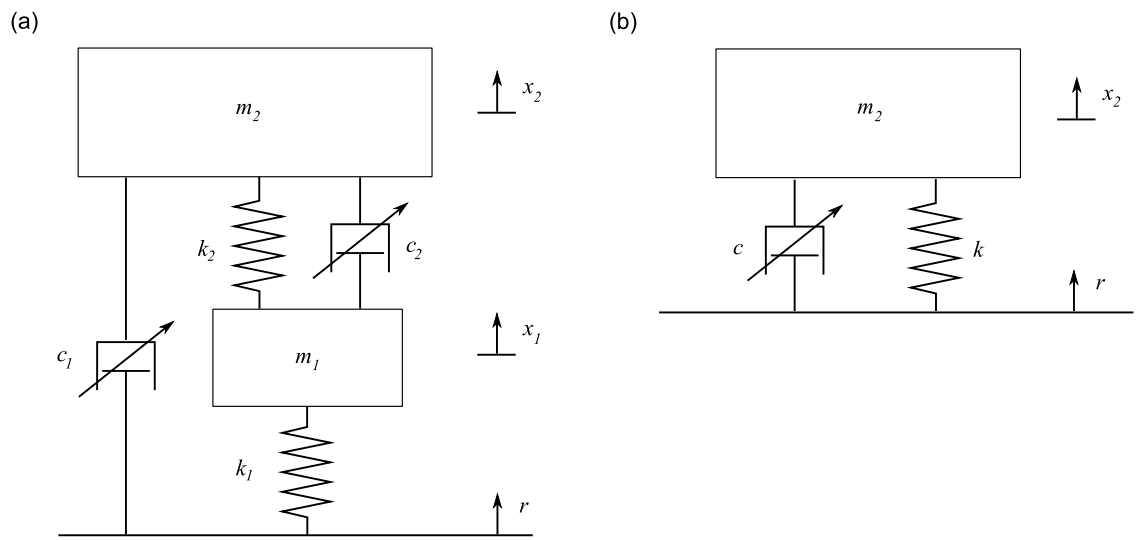


Figure 1: Mechanical models of (a) Quasi-active suspension system (b) Semi-active suspension system

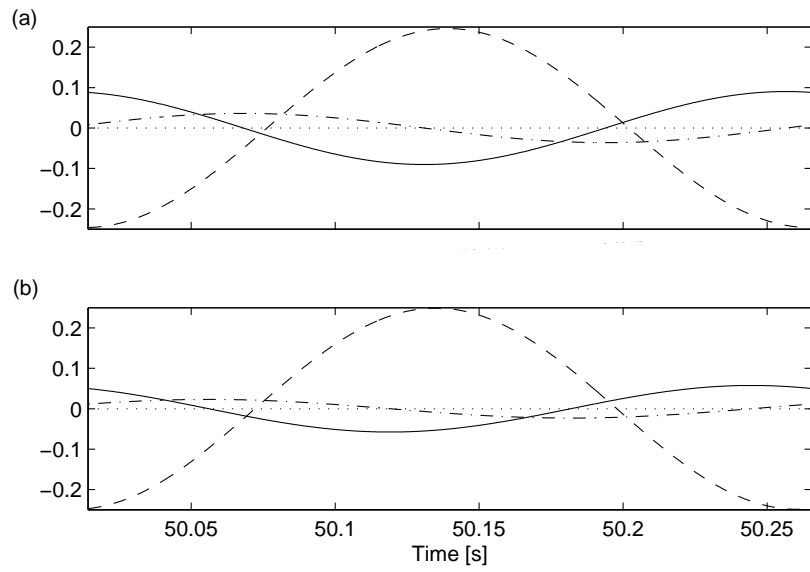


Figure 2: Steady state passive response for (a) $c_1 = c_2 = c_{min}$; (b) $c_1 = c_2 = c_{max}$:
 $-\cdot-\cdot-$ $10(x_2 - x_1)$ [m], $---$ $(\dot{x}_2 - \dot{r})$ [m/s], $---$ $(\dot{x}_2 - \dot{x}_1)$ [m/s].

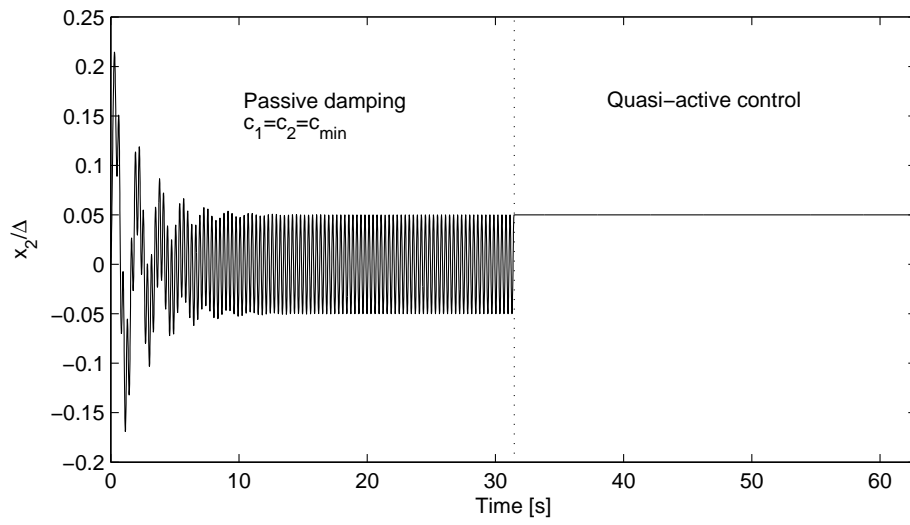


Figure 3: Controlled displacement transmissibility

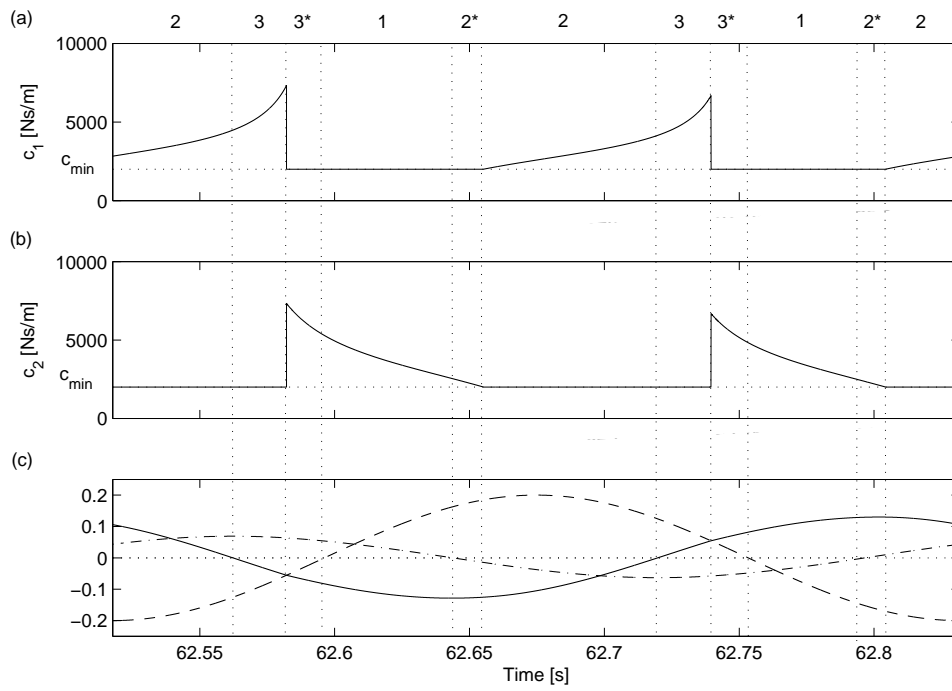


Figure 4: Steady-state controlled response (a) c_1 damping coefficient, (b) c_2 damping coefficient, (c) Damper velocities and k_2 displacement;
 \cdots $10(x_2 - x_1)$ [m], $---$ $(\dot{x}_2 - \dot{r})$ [m/s], $---$ $(\dot{x}_2 - \dot{x}_1)$ [m/s].

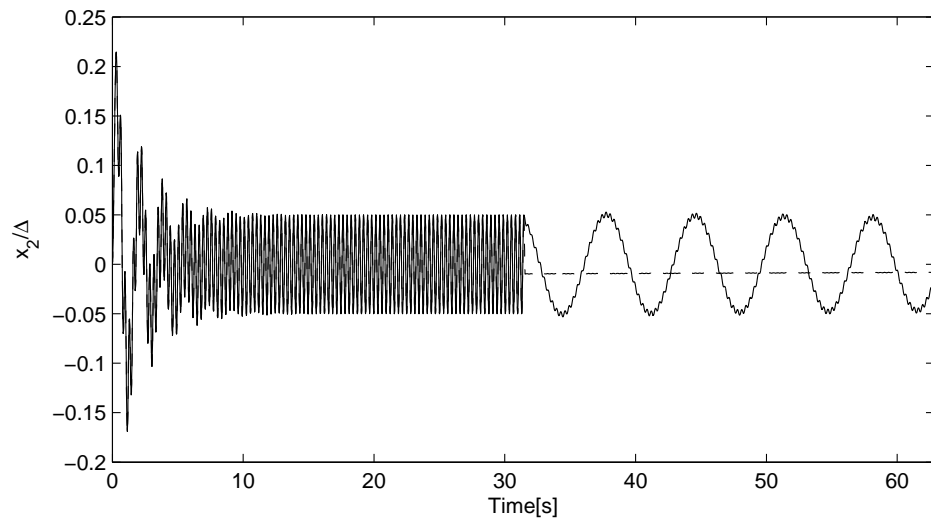


Figure 5: Controlled displacement for $\epsilon = 0.05$;

— Quasi-active control, - - - Quasi-active + closed loop control.

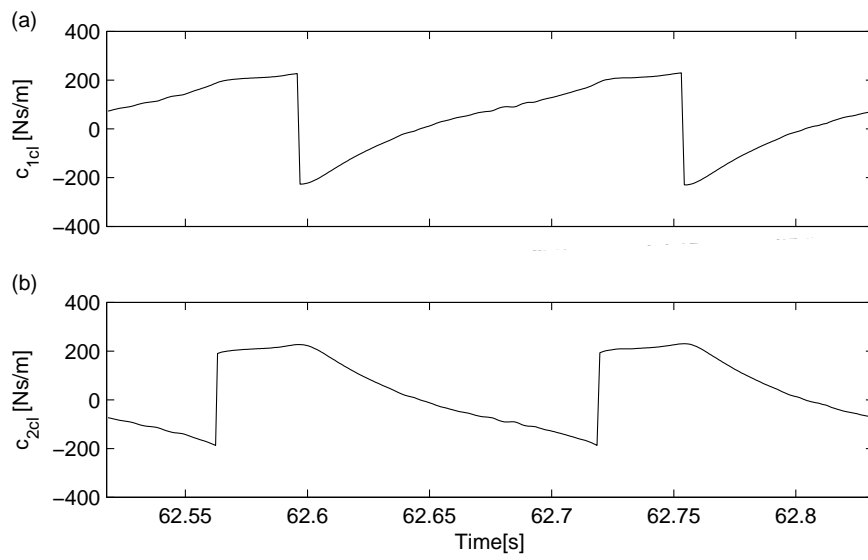


Figure 6: Closed-loop control terms for $\epsilon = 0.05$; (a) c_1 closed-loop coefficient (b) c_2 closed-loop coefficient.

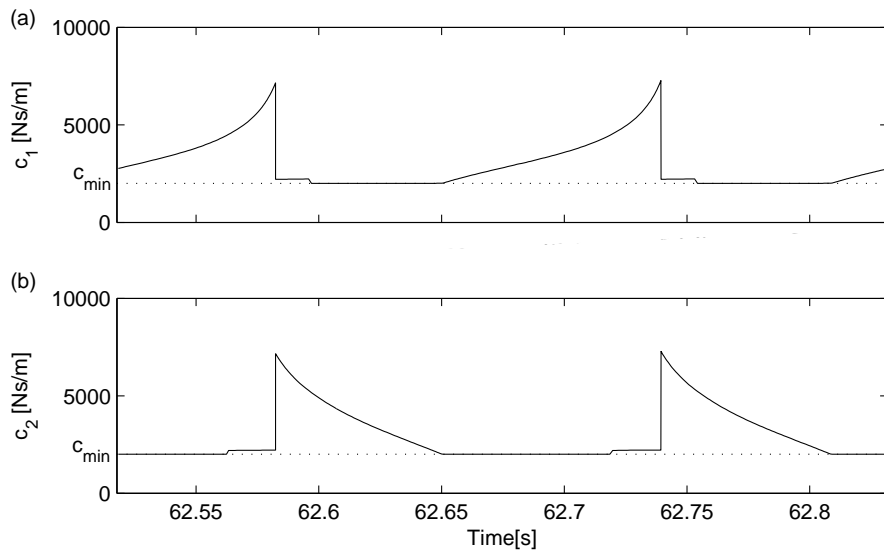


Figure 7: Controlled damping coefficients for $\epsilon = 0.05$, including quasi-active and closed-loop components (a) c_1 coefficient (b) c_2 coefficient.

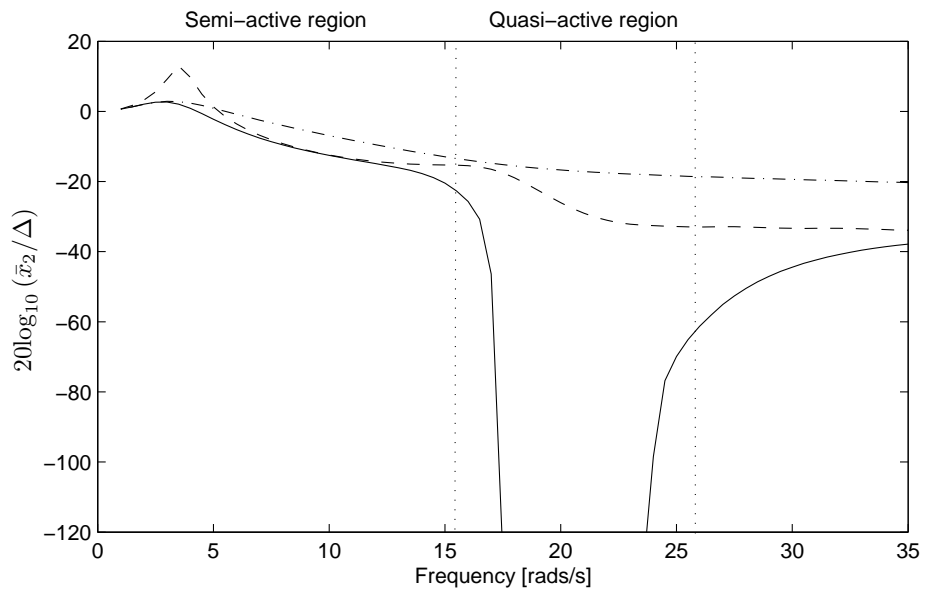


Figure 8: Displacement transmissibility; — Quasi-active control,
 - · - · - Passive damping ($c_1 = c_2 = c_{max}$), - - - Passive damping ($c_1 = c_2 = c_{min}$).

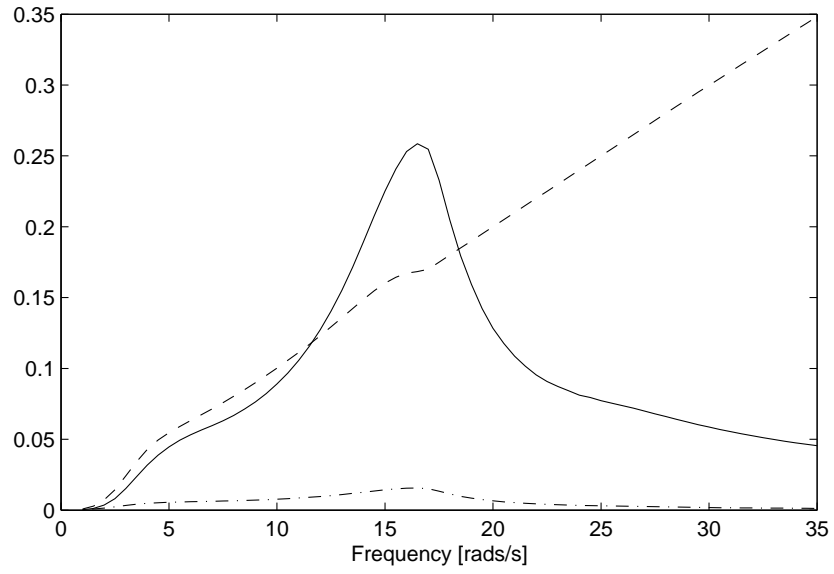


Figure 9: Controlled frequency response of k_2 displacement and damper velocity amplitudes; — $(\dot{x}_2 - \dot{x}_1)$ [m/s], - - - $(\dot{x}_2 - \dot{r})$ [m/s], - · - · - $(x_2 - x_1)$ [m].

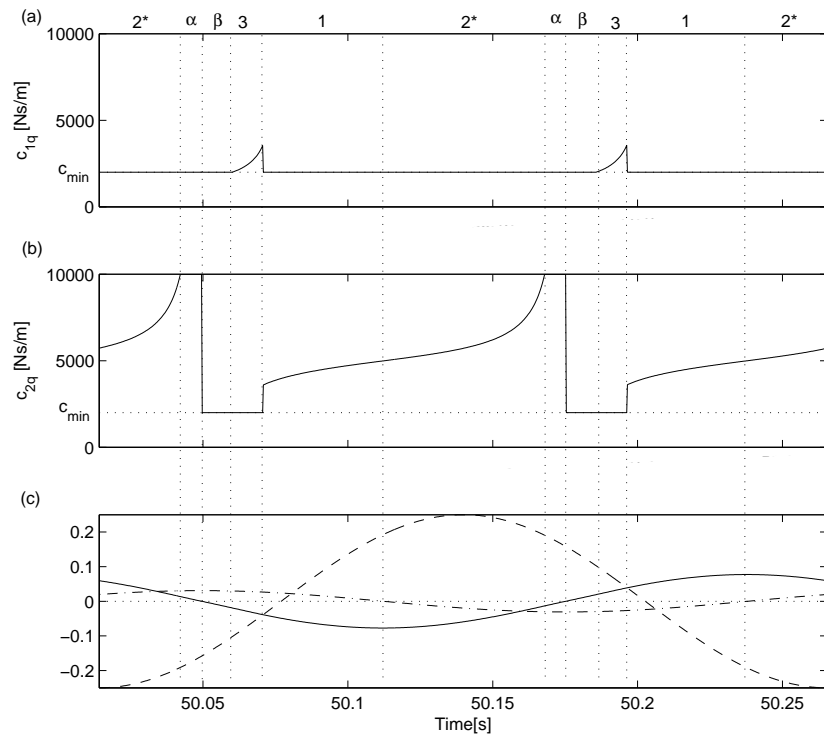


Figure 10: Steady-state controlled response at $\Omega = 25\text{rad/s}$ (a) c_{1q} damping coefficient, (b) c_{2q} damping coefficient, (c) Damper velocities and k_2 displacement; $\dots\dots\dots$ $10(x_2 - x_1)$ [m], $-\ - -$ $(\dot{x}_2 - \dot{r})$ [m/s], --- $(\dot{x}_2 - \dot{x}_1)$ [m/s].

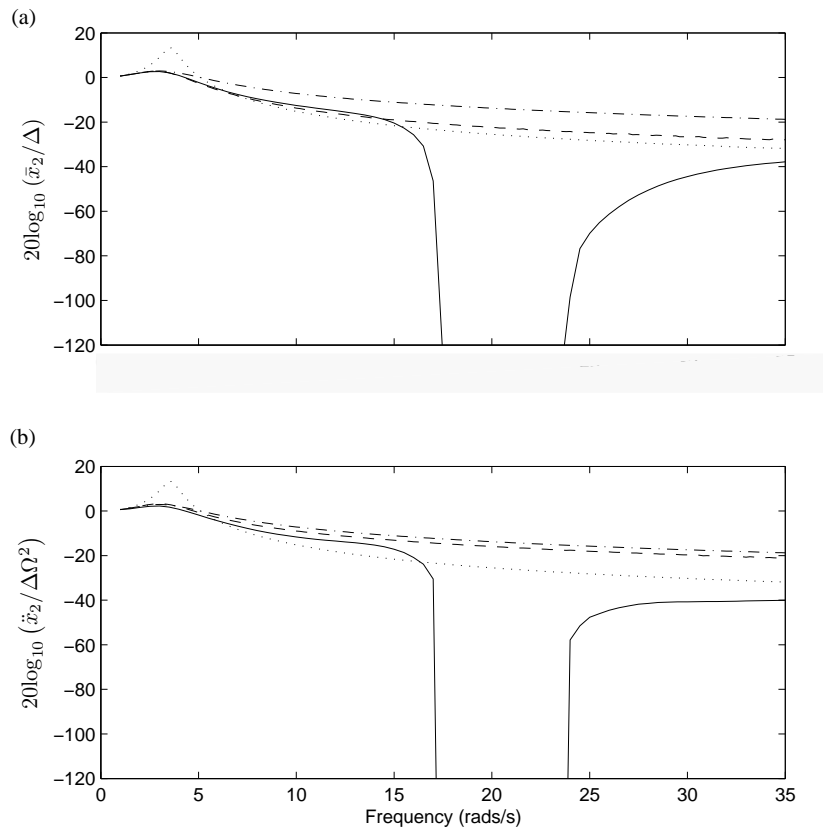


Figure 11: Steady-state frequency response of (a) displacement transmissibility (b) acceleration transmissibility;

— Quasi-Active, - · - · - Single DOF passive $c = 10,000\text{Ns/m}$,
 · · · · · Single DOF passive $c = 2,000\text{Ns/m}$, - - - Sky-hook.

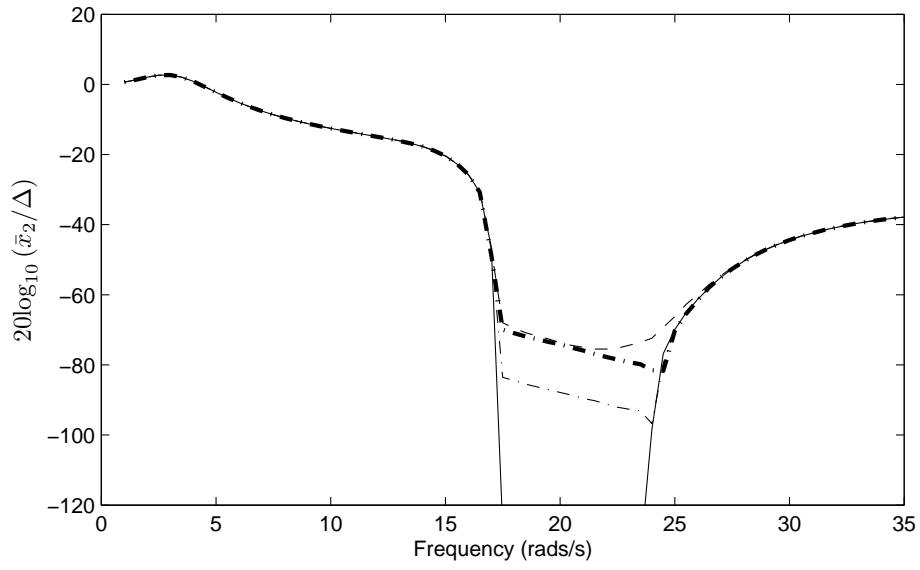


Figure 12: Displacement transmissibility of quasi-active suspension system;
 — $\epsilon = 0$, - · - · - $\epsilon = 0.01$, - - - - $\epsilon = 0.05$, - - - $\epsilon = -0.05$.

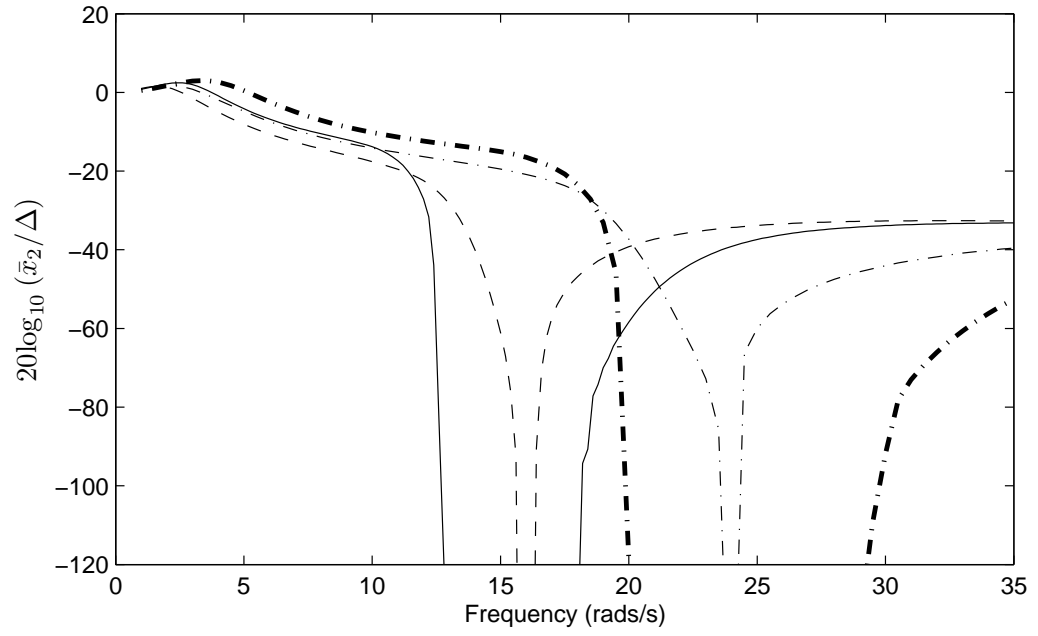


Figure 13: Displacement transmissibility of quasi-active suspension system;

- · - · - $m_1 = 250\text{kg}$, $k_1 = 47\text{kN/m}$, $k_2 = 50\text{kN/m}$,
- - - $m_1 = 375\text{kg}$, $k_1 = 25\text{kN/m}$, $k_2 = 46\text{kN/m}$,
- · - · - $m_1 = 500\text{kg}$, $k_1 = 94\text{kN/m}$, $k_2 = 91\text{kN/m}$,
- $m_1 = 750\text{kg}$, $k_1 = 51\text{kN/m}$, $k_2 = 64\text{kN/m}$.

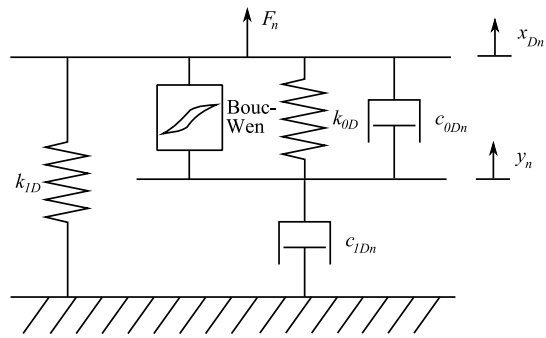


Figure 14: Mechanical model of magnetorheological damper [13]

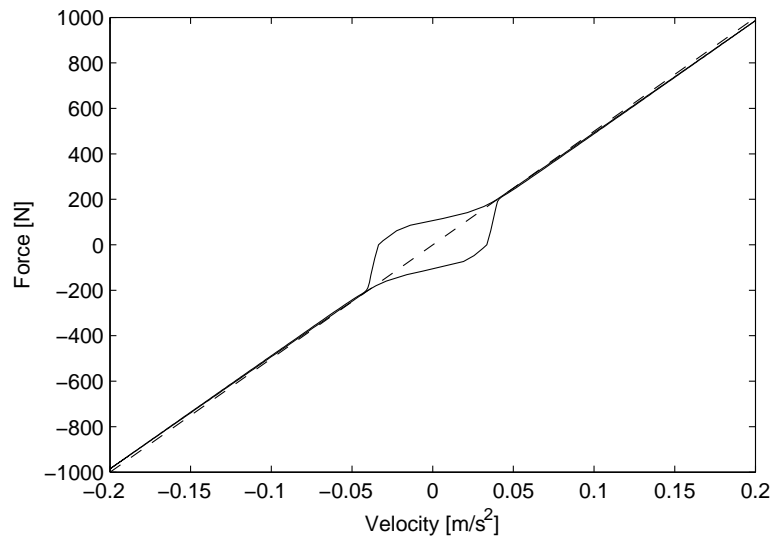


Figure 15: Force-velocity response of feedback linearised MR damper;
——— Achieved force, - - - Demanded force

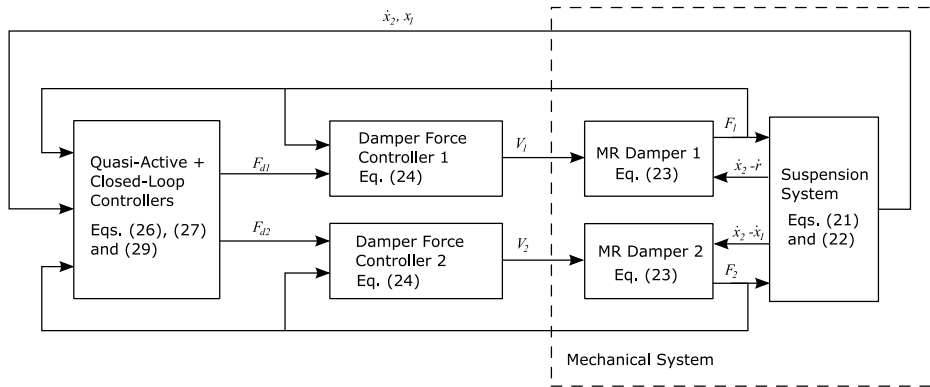


Figure 16: Illustration of control and mechanical systems.

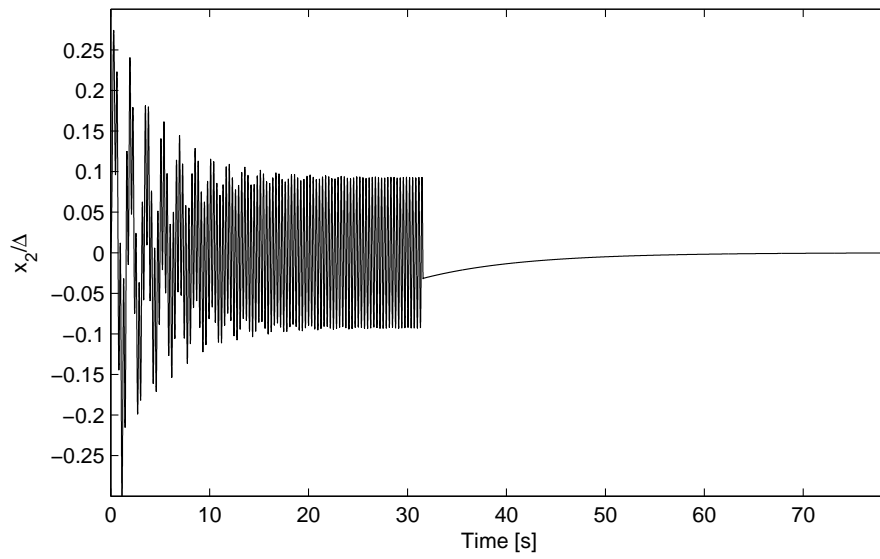


Figure 17: Controlled displacement of quasi-active MR suspension system

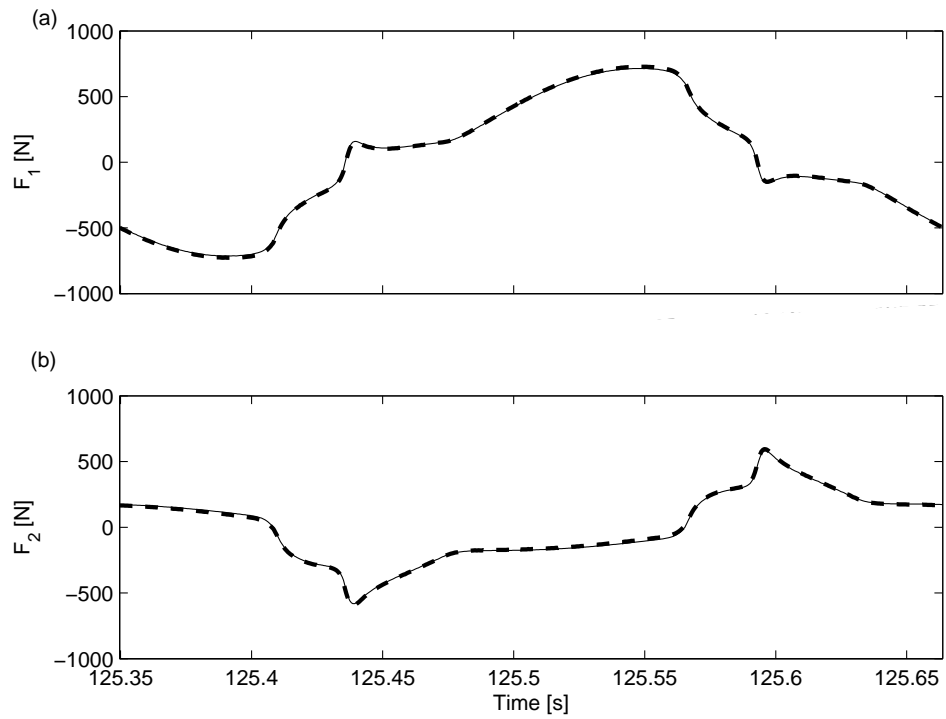


Figure 18: Steady-state demanded and achieved damper forces of quasi-active MR suspension system for $\Omega = 20 \text{ rad/s}$

(a) MR Damper 1; — F_1 , - - - F_{d1} (b) MR damper 2; — F_2 , - - - F_{d2} .

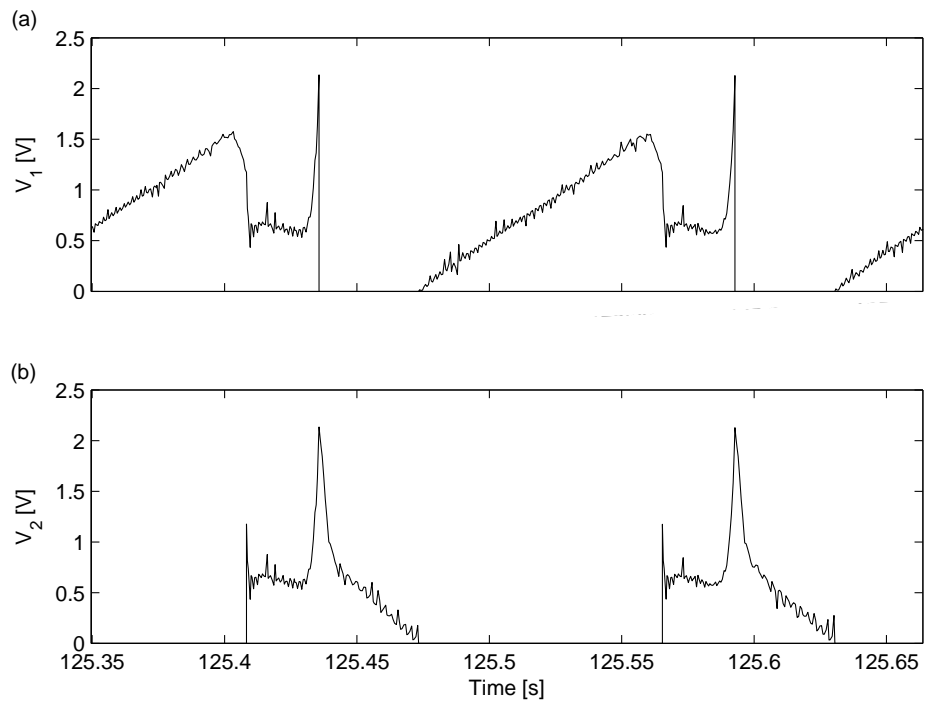


Figure 19: Steady-state damper control voltages of quasi-active MR suspension system for $\Omega = 20\text{rad/s}$ (a) V_1 (b) V_2 .

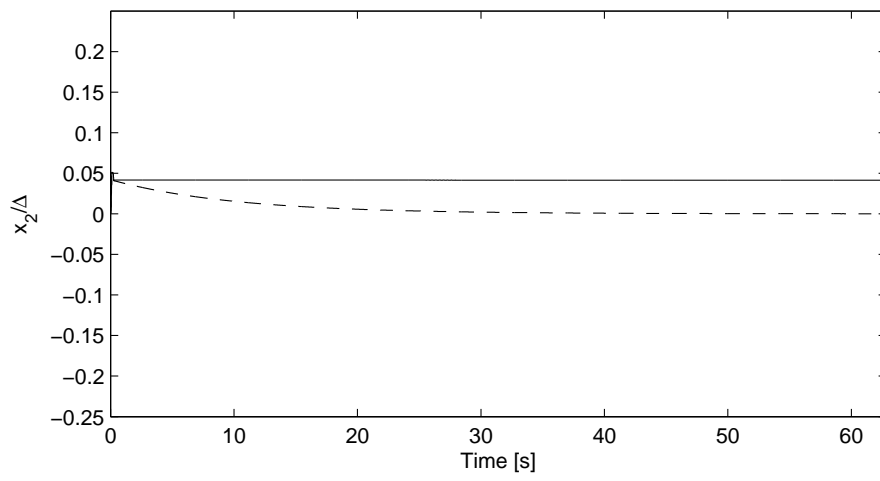


Figure 20: Controlled displacement of quasi-active MR suspension system from zero initial conditions for $\Omega = 20\text{rads/s}$; - - - Full control, ——— Proportional closed-loop control omitted.

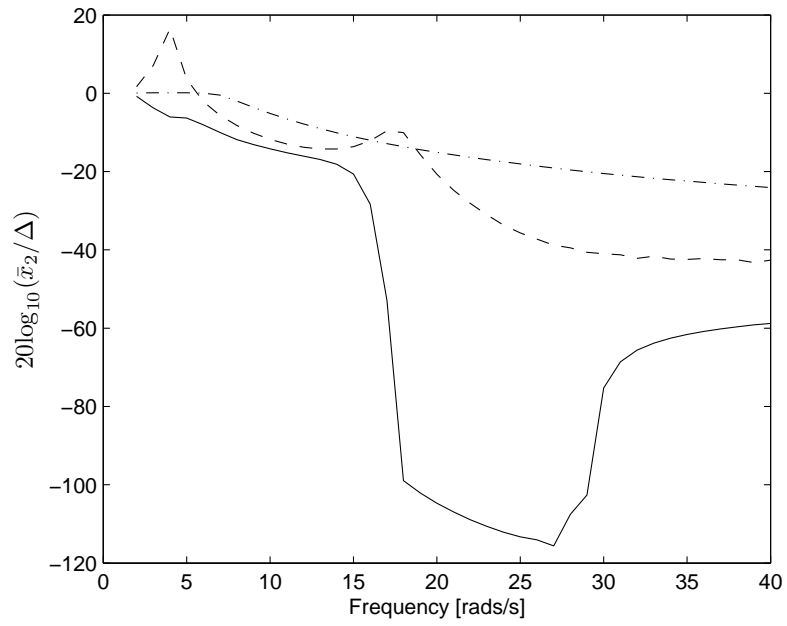


Figure 21: Displacement transmissibility of MR suspension system;
 — Quasi-active control, - - - Passive, $V_1 = V_2 = V_{min}$, - · - · - Passive, $V_1 = V_2 = V_{max}$.

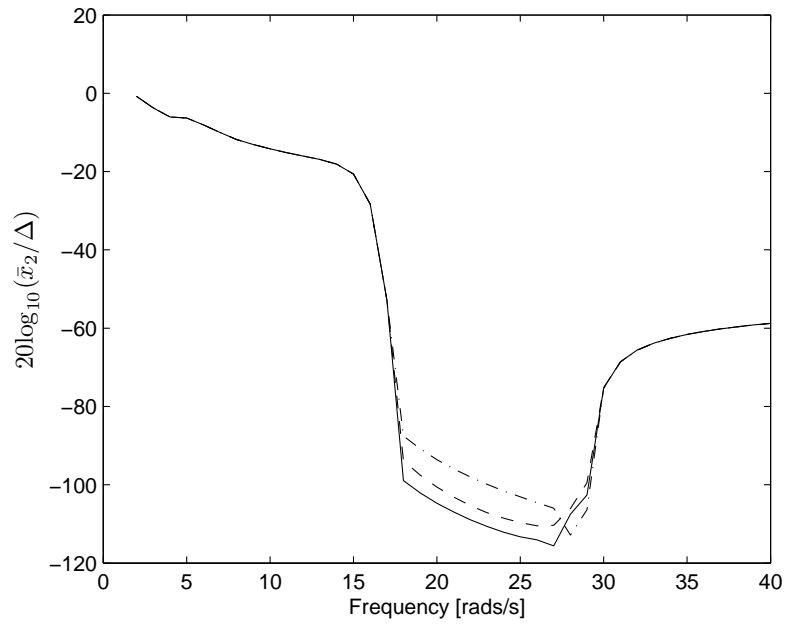


Figure 22: Displacement transmissibility of quasi-active MR suspension system;
 — $\epsilon = 0$, - - - $\epsilon = 0.05$, - · - · $\epsilon = -0.05$.

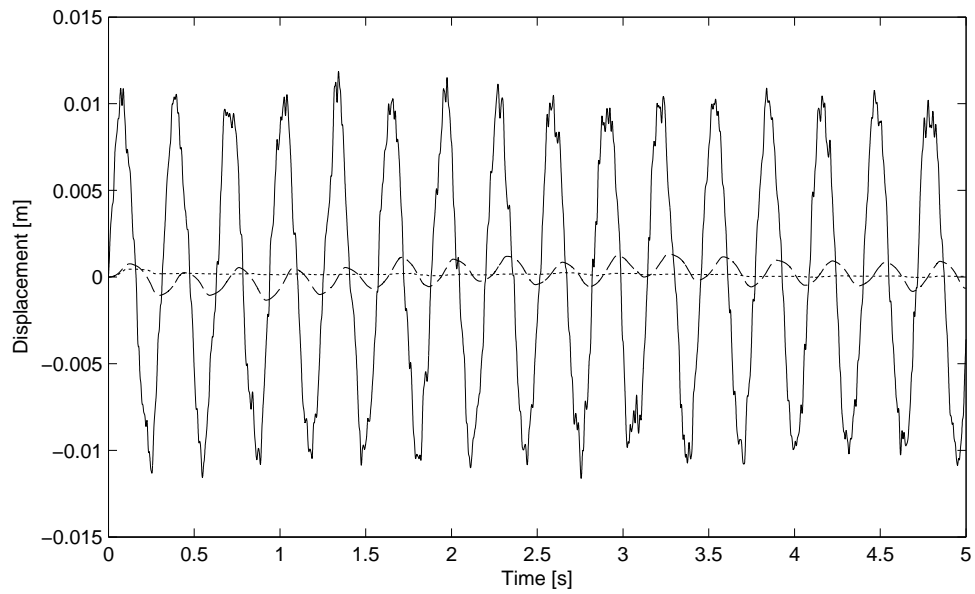


Figure 23: Response to excitation of 20 rad/s and higher frequency stochastic component; — base excitation r , - - - x_2 displacement of MR sky-hook system, ······ x_2 displacement of MR quasi-active system.

List of Tables

1	MR damper model parameters [11]	60
---	---	----

Parameter	Value	Parameter	Value
c_{0a}	784 Ns/m	α_a	12441 N/m
c_{0b}	1803 Ns/Vm	α_b	38430 N/Vm
k_{0D}	3610 N/m	γ	136320 m^{-2}
c_{1a}	14649 Ns/Vm	μ	2059020 m^{-2}
c_{1b}	34622 Ns/Vm	A	58
k_{1D}	840 N/m	k	2
x_0	0	η	190 s^{-1}
V_{min}	0V	V_{max}	3V

Table 1: MR damper model parameters [11]